Localization of Subunits D, E, and G in the Yeast V-ATPase Complex Using Cysteine-Mediated Cross-Linking to Subunit B†

Yoichiro Arata,‡ James D. Baleja,§ and Michael Forgac*,‡

Departments of Physiology and Biochemistry, Tufts University School of Medicine, 136 Harrison Avenue, Boston, Massachusetts 02111

Received June 4, 2002; Revised Manuscript Received July 12, 2002

ABSTRACT: Using a combination of cysteine mutagenesis and covalent cross-linking, we have identified subunits in close proximity to specific sites within subunit B of the vacuolar (H^+)-ATPase (V-ATPase) of yeast. Unique cysteine residues were introduced into subunit B by site-directed mutagenesis, and the resultant V-ATPase complexes were reacted with the bifunctional, photoactivatable maleimide reagent 4-(*N*-maleimido)benzophenone (MBP) followed by irradiation. Cross-linked products were identified by Western blot using subunit-specific antibodies. Introduction of cysteine residues at positions Glu^{106} and Asp^{199} led to cross-linking of subunits B and E, at positions Asp^{341} and Ala^{424} to cross-linking of subunits B and D, and at positions Ala^{15} and Lys^{45} to cross-linking of subunits B and G. Using a molecular model of subunit B constructed on the basis of sequence homology between the V- and F-ATPases, the X-ray coordinates of the F_1-ATPase, and energy minimization, Glu^{106}, Asp^{199}, Ala^{15}, and Lys^{45} are all predicted to be located on the outer surface of the complex, with Ala^{15} and Lys^{45} located near the top of the complex furthest from the membrane. By contrast, Asp^{341} and Ala^{424} are predicted to face the interior of the A_3B_3 hexamer. These results suggest that subunits E and G form part of a peripheral stalk connecting the V_1 and V_0 domains whereas subunit D forms part of a central stalk. Subunit D is thus the most likely homologue to the γ subunit of F_1, which undergoes rotation during ATP hydrolysis and serves an essential function in rotary catalysis.

The vacuolar (H^+)-ATPases (V-ATPases)[1] are ATP-dependent proton pumps present in eukaryotic cells that function both to acidify intracellular compartments and, in certain cases, to pump protons across the plasma membrane (*1*−*8*). Acidification of intracellular compartments is essential for such processes as ligand-receptor dissociation following receptor-mediated endocytosis, intracellular targeting of newly synthesized lysosomal enzymes, coupled transport of small molecules such as neurotransmitters, and the processing and degradation of macromolecules in secretory granules and lysosomes. Proton transport across the plasma membrane of osteoclasts, renal intercalated cells, macrophages, and insect goblet cells has been shown to be necessary for bone resorption, renal acidification, cytoplasmic pH homeostasis, and potassium secretion, respectively (*9*−*12*).

The V-ATPases are composed of two functional domains, V_1 and V_0 (*1*−*8*). The V_1 domain is a 640 kDa peripheral complex containing eight different subunits (subunits A−H) of molecular mass 70−14 kDa that is responsible for ATP hydrolysis. The catalytic nucleotide binding sites are located on the 70 kDa A subunit (present in three copies per complex), whereas the 60 kDa B subunit (also present in three copies) contains so-called "noncatalytic" sites of unknown function. The V_0 domain is a 260 kDa integral complex composed of five subunits (subunits a, d, c, c′, and c″) of molecular mass 100−17 kDa that is responsible for proton translocation.

The V-ATPases are structurally and evolutionarily related to the ATP synthases (or F-ATPases) of mitochondria, chloroplasts, and bacteria, which normally function in ATP synthesis (*13*−*18*). Thus, the A and B subunits of the V-ATPase are homologous to the β and α subunits of F_1, respectively (*19*, *20*), whereas the proteolipid subunits of the two complexes are also homologous (*21*, *22*). The X-ray crystal structure of F_1 reveals a hexamer of alternating α and β subunits surrounding a central cavity containing the highly α-helical γ subunit (*23*−*25*). F_1 is attached to F_0 by both a central stalk, composed of the γ and ϵ subunits (*25*, *26*), and a peripheral stalk, containing the δ subunit and the soluble portion of subunit b of the F_0 domain (*27*, *28*). F_0 is composed of a ring of c subunits with the a and b subunits to one side (*15*, *29*).

The V-ATPases have been proposed to operate by a rotary mechanism similar to that demonstrated for F_1F_0 (*30*, *31*). In this mechanism, ATP hydrolysis at the catalytic sites on the β subunits drives rotation of the central γ subunit of F_1, which in turn drives rotation of the ring of c subunits in F_0.

† This work was supported in part by National Institutes of Health Grant GM34478 (to M.F.), Research Project Grant 00-087-01 from the American Cancer Society (to J.D.B.), and a fellowship from the Uehara Memorial Foundation of Japan (to Y.A.). *E. coli* strains were provided through National Institutes of Health Grant DK34928.

* To whom correspondence should be addressed. Phone: (617) 636-6939. Fax: (617) 636-0445. E-mail: michael.forgac@tufts.edu.

‡ Department of Physiology.

§ Department of Biochemistry.

[1] Abbreviations: V-ATPase, vacuolar proton-translocating adenosine 5-triphosphatase; F-ATPase, F_1F_0 ATP synthase; MBP, 4-(*N*-maleimido)benzophenone; ACMA, 9-amino-6-chloro-2-methoxyacridine; PAGE, polyacrylamide gel electrophoresis.

10.1021/bi0262449 CCC: $22.00
Published on Web 08/23/2002

The c subunit ring rotates relative to subunit a, which is held fixed relative to the $\alpha_3\beta_3$ hexamer by the peripheral stalk (or stator). It is thought to be the movement of buried carboxyl groups on the c subunit ring relative to static charges and access channels located on subunit a that results in unidirectional, proton movement through F_0. ATP-dependent rotation of both the γ subunit and the ring of c subunits has been demonstrated (*32*−*37*). As with F_1F_0 (*38*), the V_1 and V_0 domains are connected by both a central and a peripheral stalk (*39*, *40*), although the subunit composition of these stalks has not been established.

To address the arrangement of subunits in the V-ATPase complex, we have employed a combination of site-directed mutagenesis to introduce unique cysteine residues into subunit B and covalent cross-linking using a photoactivatable sulfhydryl reagent. A molecular model of subunit B was constructed on the basis of sequence homology between the nucleotide binding subunits of the V- and F-ATPases, the X-ray coordinates of F_1, and energy minimization (*41*). This model was shown to accurately predict the identity of a number of residues present at the nucleotide binding site on the B subunit (*41*). Using this model, specific residues were selected for mutation to cysteine on the basis of their predicted orientation in the complex. We have previously shown that four cysteine residues predicted to be oriented toward the outer surface of the V-ATPase complex lead to cross-linking of subunits B and E, suggesting that subunit E is located on the periphery of the complex (*42*). In the current paper we have extended this analysis both by using additional cysteine mutants of the B subunit and by employing additional subunit-specific antibodies that have allowed us to identify cross-linked products containing subunits D and G as well as subunits B and E. The results support a peripheral location for both subunits E and G, whereas subunit D appears to be located within the interior of the complex.

EXPERIMENTAL PROCEDURES

Materials and Strains. Zymolyase 100T was obtained from Seikagaku America, Inc. Concanamycin A was purchased from Fluka Chemical Corp. 9-Amino-6-chloro-2-methoxyacridine (ACMA) was obtained from Molecular Probes, Inc. SDS, nitrocellulose membranes (0.45 μm pore size), Tween 20, horseradish peroxidase-conjugated goat anti-rabbit IgG, and horseradish peroxidase-conjugated goat anti-mouse IgG were from Bio-Rad. 4-(*N*-Maleimido)benzophenone (MBP) and most other chemicals were obtained from Sigma. The chemiluminescence substrate for horseradish peroxidase was from KPL Laboratories.

In yeast subunit B is encoded by the *VMA2* gene. The yeast *VMA2*-deleted strain, SF838-5AV1 (*vat2-Δ1::LEU2*), and pCY41 (*VMA2* in pBluescript) have been described previously (*43*, *44*) and were kind gifts from Dr. Patricia Kane, Upstate Medical University.

Antibodies. Anti-Vma1p, anti-Vma2p, and anti-Vph1p are all mouse monoclonal antibodies and were purchased from Molecular Probes, Inc. Anti-Vma4p is a rabbit polyclonal antiserum and was a gift from Dr. Daniel Klionsky, University of Michigan. Anti-Vma8p and anti-Vma10p are also rabbit polyclonal antisera and were gifts from Dr. Tom Stevens, University of Oregon.

Construction of Mutants. Site-directed mutants were constructed using the Altered Sites II in vitro mutagenesis system (Promega) following the manufacturer's protocol (*42*). Additional mutations were made using the mutant *VMA2* encoding the Cys-less form of subunit B (C188S) in pAlter-1 as a template and mutagenic oligonucleotide primers with the sequences described previously (*42*) except for the following (substitutions are italic):

E106C,
5′-ATTCCTGTGTCT*TGT*GACATGTTGGGT-3′

A424C,
5′-GTCGGTGAAGAG*TGT*TTATCCATCGAA-3′

Transformation of yeast and selection of transformants on Ura^- plates were carried out as described previously (*41*). The mutants were then tested for growth on pH 7.5 or 5.5 yeast extract−peptone−dextrose plates buffered with 50 mM KH_2PO_4 and 50 mM succinic acid (*44*).

Isolation of the Vacuolar Membranes. Vacuolar membranes were prepared from the *vma2*Δ strain expressing the wild-type *VMA2* gene in pRS316, the pRS316 vector alone, the mutant *VMA2* gene encoding the Cys-less form of subunit B (C188S) in pRS316, or the single-cysteine-containing double mutants of *VMA2* containing the C188S mutation and the mutations listed above in pRS316 as described previously (*41*).

Covalent Cross-Linking of the V-ATPase Using MBP. Vacuolar membranes were prepared from the *vma2*Δ strain expressing the wild-type *VMA2* gene in pRS316, the pRS316 vector alone, the mutant *VMA2* gene encoding the Cys-less form of subunit B (C188S) in pRS316, or the single-cysteine-containing double mutants of *VMA2* containing the C188S mutation and the mutations described above in pRS316. Covalent cross-linking using MBP was performed as described previously (*42*). Briefly, vacuolar membrane vesicles (50−200 μg of protein) were washed in phosphate-buffered saline and 2 mM EDTA (pH 7.2), resuspended in 100 μL of the same buffer (plus protease inhibitors), and reacted with MBP at 1 mM for 30 min at 23 °C in the dark. Unreacted MBP was quenched by addition of 10 mM dithiothreitol, and the samples were irradiated for 5 min at 4 °C with a long-wavelength ultraviolet light.

Analysis of Cross-Linked Products. After covalent cross-linking with MBP, cross-linked products were analyzed in one of two ways. For detection of cross-linking between subunits B and G, we used the method employed in our previous study (*42*). Vesicles (15 μg of protein/lane) were directly separated by SDS−PAGE on 10% acrylamide gels according to the method of Laemmli (*45*). Alternatively, for analysis of cross-linking between subunit B and subunits E and D, vesicles were solubilized with 2% $C_{12}E_9$ and the V-ATPase complex was immunoprecipitated using protein A−Sepharose and the mouse monoclonal antibody 13D11 specific for subunit B prior to separation by SDS−PAGE on 7.5% acrylamide gels. In all cases, gel electrophoresis was followed by transfer to nitrocellulose and Western blotting using antibodies specific for subunit B, D, E, or G as previously described (*42*). The advantages of analyzing cross-linked products using vesicles is simplicity and cost (i.e., eliminating the immunoprecipitation step), whereas the advantage of including immunoprecipitation prior to Western

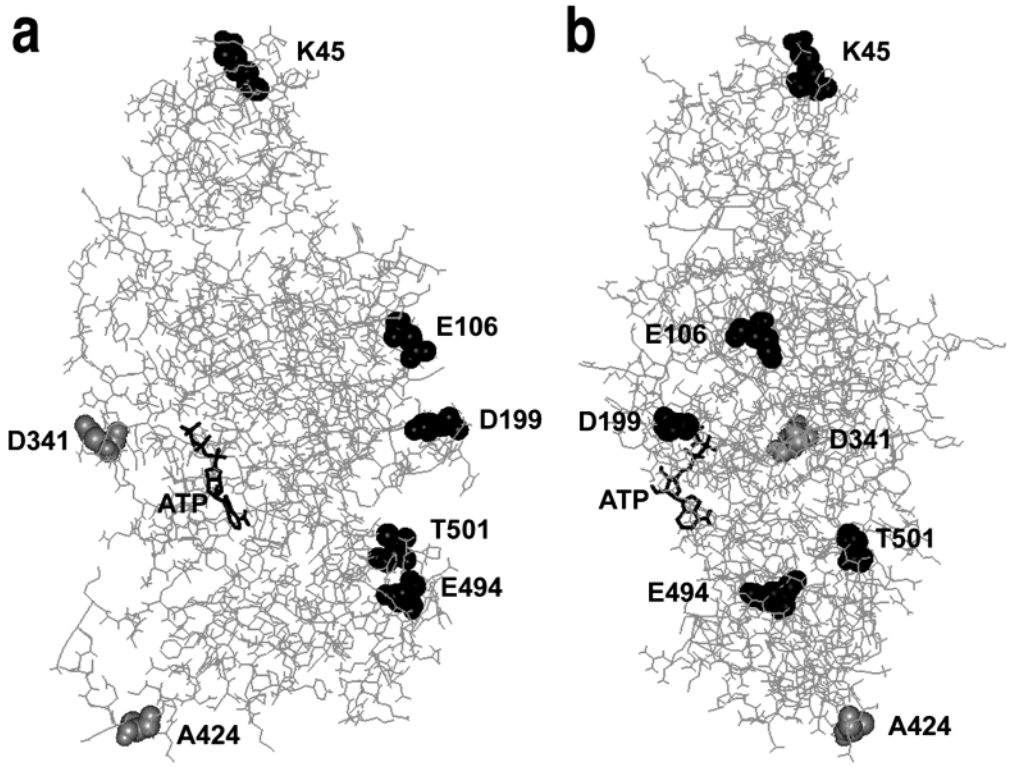

FIGURE 1: Structural model of subunit B of the V-ATPase. Shown is an energy-minimized model of the B subunit of the V-ATPase based upon the X-ray crystal structure of the bovine mitochondrial F_1-ATPase (*23*) and sequence alignment of the V- and F-ATPase nucleotide binding subunits (see the Experimental Procedures). The structure is oriented such that the region furthest from the membrane is at the top. In panel a, the external surface of V_1 is shown on the right, while the region oriented toward the interior of the V_1 complex is shown on the left. In panel b, the molecule is rotated 90° about the vertical axis such that the external surface is facing out of the page. Externally oriented residues selected for mutagenesis to cysteine are shown in black, while internally oriented residues are shown in gray. Residue Ala^{15} is not shown because the structure for this portion of the α subunit was not available, although it is likely to reside near the top of the molecule. The remainder of the A_3B_3 hexamer is not shown for clarity although the entire hexamer was used in the energy minimization.

blot analysis is the generally cleaner nature of the blots due to elimination of most nonspecifically reacting bands.

Modeling of the V-ATPase B Subunit. A model for the A_3B_3 hexamer of the V_1 domain was created from the X-ray crystal structure of bovine mitochondrial F_1-ATPase (*23*) as previously described (*41*, *42*). Alignment of the amino acid sequences was carried out using the Genetics Computer Group (GCG) sequence analysis software package, and energy minimization was performed using X-PLOR.

Other Procedures. ATPase activity was measured using a coupled spectrometric assay as previously described (*41*). ATP-dependent proton transport was measured by fluorescence quenching using the probe ACMA as described previously (*41*) using a Perkin-Elmer LS50B spectrofluorimeter. Activities were measured in the absence or presence of 1 μM concanamycin A, a specific inhibitor of the V-ATPase (*46*). Protein concentrations were determined by the method of Bradford (*47*).

RESULTS

Strategy and Construction of B Subunit Mutants Containing Unique Cysteine Residues. To define the location of subunits within the V-ATPase complex, unique cysteine residues were introduced into the B subunit and used as sites of attachment of the photoactivatable cross-linker MBP. Residues were selected for mutation to cysteine on the basis of the molecular model of subunit B shown in Figure 1. This model was constructed using the available high-resolution structural data on F_1 (*23*), sequence homology between the nucleotide binding subunits of the V- and F-ATPases, and energy minimization as described in the Experimental Procedures. The view depicted in Figure 1a shows subunit B oriented with residues predicted to be facing the exterior of the complex (including Lys^{45}, Glu^{106}, Asp^{199}, Glu^{494}, and Thr^{501}) on the right and residues predicted to be facing the interior of the complex (including Asp^{341} and Ala^{424}) on the left. Figure 1b shows a view rotated 90° around the vertical axis, with the exterior facing residues projected out of the page. In both views the top of the molecule corresponds to the point furthest from the membrane. The location of Ala^{15}, while not precisely defined by the model because of limits on the available X-ray data, is likely to be near the top of the molecule.

Mutations were constructed in the *VMA2* gene in yeast. The wild-type *VMA2* gene contains a single endogenous cysteine residue at position 188, which we have previously shown can be replaced with serine to give a V-ATPase complex possessing >90% of the wild-type activity (*41*). Using this Cys-less form of the B subunit as the starting point, unique cysteine residues were then introduced at each of the indicated positions. The mutant *vma2* cDNAs were subcloned into the yeast shuttle vector pRS316 and expressed in a *vma2*Δ strain lacking the endogenous *VMA2* gene.

Effect of B Subunit Mutations on V-ATPase Assembly and Activity. The effect of each mutation on the stability of the B subunit and assembly of the V-ATPase complex was

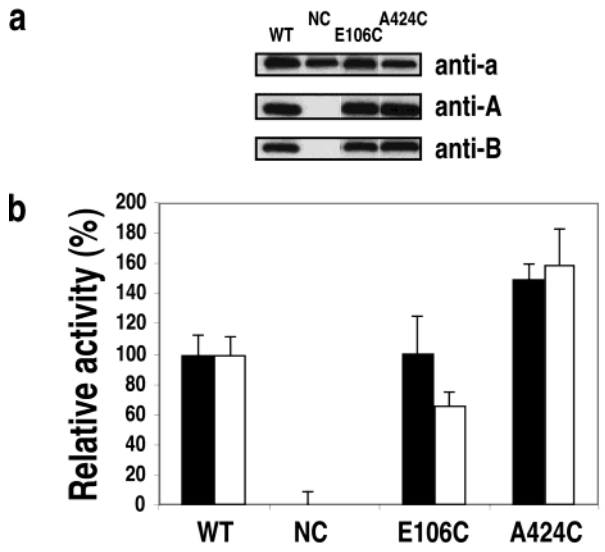

FIGURE 2: Effect of cysteine mutations E106C and A424C of *VMA2* on the assembly and activity of V-ATPase complexes. (a) Vacuolar membranes (5 μg of protein) were prepared from the *vma2*Δ strain expressing the wild-type *VMA2* gene (WT), the vector alone (NC, negative control), or the single-cysteine-containing double mutants of *VMA2* containing the C188S mutation and the indicated mutation. The proteins were separated by SDS−PAGE on a 10% acrylamide gel and transferred to nitrocellulose. Western blotting was then performed using the monoclonal antibodies 8B1F3, 13D11, and 10D7 against subunits A, B, and a, respectively, as described in the Experimental Procedures. (b) Vacuolar membranes were prepared from the strains described in panel a and assayed for concanamycin A-sensitive ATPase activity (5 μg of protein, shaded bars) and concanamycin A-sensitive, ATP-dependent proton transport (1 μg of protein, open bars) as described previously (*42*).

assessed by Western blot analysis performed on vacuoles isolated from each of the mutant strains using antibodies specific for subunits A and B. It has previously been shown that disruption of V-ATPase assembly by loss of any of the V-ATPase subunits (except subunit H) leads to decreased levels of all of the V_1 subunits on the vacuolar membrane (*48*). We have previously analyzed six of the eight mutations employed in this study, including A15C, K45C, D199C, D341C, E494C, and T501C, and shown that they all show normal expression levels and assembly relative to those of the wild-type B subunit (*42*). In addition, as shown in Figure 2a, vacuoles isolated from the strains expressing E106C and A424C show wild-type levels of both subunits A and B, indicating normal expression of the B subunit and assembly with the remainder of the V-ATPase complex.

We determined the effect of the B subunit mutations on ATPase activity and proton transport. Concanamycin A-sensitive ATPase activity and ATP-dependent ACMA quenching were measured on vacuoles isolated from each of the mutant strains. The previously characterized mutants (A15C, K45C, D199C, D341C, E494C, and T501C) all showed greater than 50% of the wild-type levels of both proton transport and ATPase activity (*42*). As shown in Figure 2b, vacuoles isolated from the strains expressing E106C and A424C show activities greater than 60% of the wild-type activity. These results suggest that the mutations introduced into the B subunit do not seriously compromise V-ATPase function. Consistent with these observations, all mutant strains show normal growth at pH 7.5 (data not shown).

Photoactivated Cross-Linking of V-ATPase Complexes Containing Mutant Forms of Subunit B. To identify V-ATPase subunits in proximity to the cysteine residues introduced into subunit B, photoactivated cross-linking was performed using MBP (*42*, *49*). MBP reacts with cysteine residues via the maleimide group and, upon irradiation, generates a highly reactive species capable of cross-linking to adjacent residues within 10 Å of the original site of reaction (*50*). We have previously shown that for the Cys-less form of subunit B, MBP results in no detectable cross-linking of subunit B to other subunits in the V-ATPase complex (*42*). Therefore, any cross-linked products containing subunit B observed for the single-cysteine-containing mutants are the result of MBP reaction in the first step with the unique cysteine residue in the B subunit. Vacuoles from cells expressing mutant forms of subunit B were reacted with MBP in the dark followed by irradiation with ultraviolet light. The V-ATPase was then solubilized with $C_{12}E_9$ and immunoprecipitated using an antibody against subunit B followed by SDS−PAGE and Western blotting using subunit-specific antibodies as described in the Experimental Procedures.

As can be seen in Figure 3, for both the E106C and D199C mutants, a cross-linked product recognized by antibodies against both subunit B and subunit E is observed. This product is seen in the presence, but not the absence, of MBP. Although the molecular mass of this cross-linked product is somewhat larger than that predicted for a B−E heterodimer (57 kDa + 27 kDa = 84 kDa), it is possible that this species may migrate aberrantly on SDS−PAGE due to cross-linking at sites near the middle of the B subunit. These results suggest that subunits B and E are in close proximity on the external surface of the complex near the middle of the B subunit. For the D199C mutant, we had previously observed a faint cross-linked product at 110 kDa in vacuoles that was recognized by both the anti-B and anti-E subunit antibodies (*42*), and had discussed the possible cause of its aberrant migration. The fact that this same cross-linked product is observed in a V-ATPase complex isolated by immunoprecipitation using an antibody against subunit B (present work) further supports the suggestion that this product results from cross-linking of subunits B and E.

By contrast, for mutants containing cysteine residues at positions 341 and 424, cross-linked products that are recognized by antibodies against both subunits B and D are observed (Figure 4). For the D341C mutant, a single band of apparent molecular mass 130 kDa reacts with both the anti-B and anti-D subunit antibodies. The lower mobility of this band relative to the predicted size of a B−D heterodimer (57 kDa + 32 kDa = 89 kDa) may again be due to cross-linking near the middle of the B subunit. For the A424C mutant, however, a series of higher molecular weight bands are observed with both the anti-B and anti-D subunit antibodies. The bands with apparent molecular mass above 173 kDa we postulate correspond to subunit D cross-linked to multiple B subunits. Because there are three copies of subunit B per complex, this type of multiple cross-linking is possible, especially if, as these results suggest, subunit D is located within a cavity surrounded by the A_3B_3 hexamer. The pair of bands centered around 105 kDa likely represent B−D heterodimeric complexes that are formed from cross-linking of subunit B to different positions on subunit D (see the Discussion). In both Figures 3 and 4, bands shown with

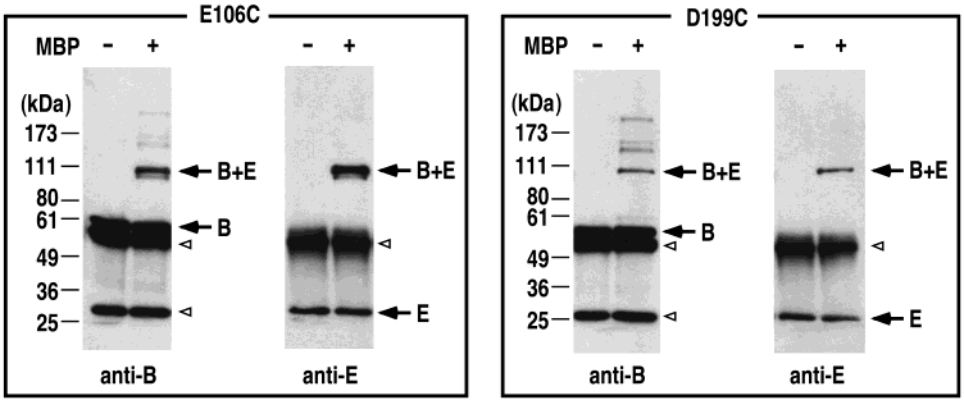

FIGURE 3: Cross-linking of V-ATPase subunits B and E using the photoactivatable sulfhydryl reagent MBP. Vacuolar membranes were prepared from the *vma2*Δ strain expressing the single-cysteine-containing double mutants of *VMA2* containing C188S and the indicated mutation and incubated in the presence (+) or absence (−) of 1 mM MBP for 30 min at 23 °C. The excess MBP was quenched by addition of 10 mM dithiothreitol, and the samples were irradiated with a long-wavelength ultraviolet lamp for 5 min at 4 °C. The membranes were then solubilized with $C_{12}E_9$, and the V-ATPase was immunoprecipitated using the monoclonal antibody 13D11 against subunit B and protein A−Sepharose. Samples were separated by SDS−PAGE using a 7.5% acrylamide gel and transferred to nitrocellulose, and Western blotting was perfomed using antibodies against Vma2p (subunit B) or Vma4p (subunit E). Indicated to the left of each panel are the molecular masses of marker proteins and to the right the positions of subunits B and E and the B−E heterodimer. The white arrowheads indicate the positions of the heavy and light chains of the antibodies used to immunoprecipitate the V-ATPase complex. The reason that the light chain is not visible in the anti-E subunit antibody blots is that the secondary antibody employed in these blots is a goat anti-rabbit antibody, which does not react strongly with the mouse monoclonal antibody against subunit B used for immunoprecipitation of the complex. By contrast, the secondary antibody employed in the anti-B subunit antibody blots is a goat anti-mouse antibody, which recognizes the immunoprecipitating mouse monoclonal antibody strongly.

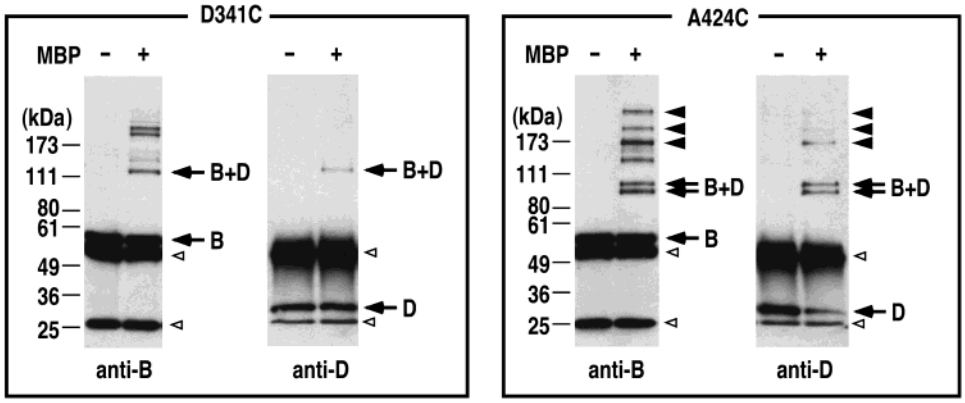

FIGURE 4: Cross-linking of V-ATPase subunits B and D using MBP. Vacuolar membranes were prepared from the *vma2*Δ strain expressing the indicated single-cysteine-containing double mutants of *VMA2* and were reacted with MBP followed by photoactivation, solubilization, immunoprecipitation, and SDS−PAGE as described in Figure 3. Western blotting was performed using antibodies against Vma2p (subunit B) or Vma8p (subunit D). Indicated to the left of each panel are the molecular masses of marker proteins and to the right the positions of subunits B and D and the cross-linked products which react with both the anti-B and anti-D subunit antibodies (see the Results). The white arrowheads indicate the positions of the heavy and light chains of the antibodies used to immunoprecipitate the V-ATPase complex.

white arrowheads represent the heavy and light chains of the antibodies used to immunoprecipitate the V-ATPase complex.

Using the simplified procedure we had employed in our previous study, in which photoactivated cross-linking of the V-ATPase in isolated vacuoles was followed immediately by SDS−PAGE and Western blot analysis (*42*), we have also observed the formation of a B−G heterodimer for both the A15C and K45C mutants (Figure 5). In this case, the observed molecular mass of the cross-linked product (70 kDa) is identical to that predicted for the sum of subunit B (57 kDa) and subunit G (13 kDa). Cross-linking is again dependent upon the presence of MBP and is not observed in the absence of irradiation (data not shown). This cross-linked product is also not observed for mutants containing cysteines at positions 106, 199, 494, and 501 (data not shown). These results suggest that subunit G is located on the external face of the complex, with at least a portion of its mass near the top of the molecule. Besides the previously characterized B−E heterodimer, the identity of other cross-linked products observed with the K45C mutant was not determined. It should be noted that, because of the very low molecular mass of subunit G (13 kDa), a significant amount of the monomeric form of subunit G may have undergone transfer through the nitrocellulose membrane during Western blotting, so the apparent efficiency of cross-linking of subunit G may be somewhat overestimated.

DISCUSSION

The results of the current study employing cysteine mutagenesis and photoactivated cross-linking suggest that subunits E and G are located on the periphery of the V-ATPase complex, with subunit G located near the top of the molecule furthest from the membrane. The E subunit

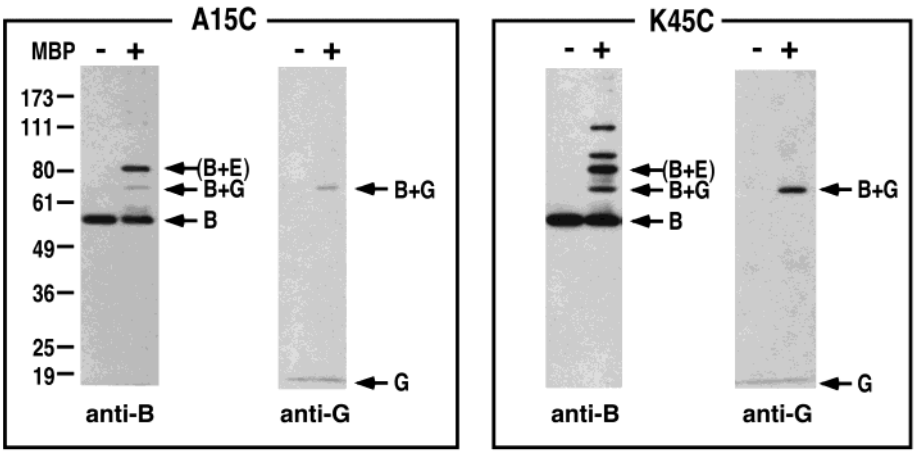

FIGURE 5: Cross-linking of V-ATPase subunits B and G using MBP. Vacuolar membranes were prepared from the *vma2*Δ strain expressing the indicated single-cysteine-containing double mutants of *VMA2* and incubated in the presence (+) or absence (−) of 1 mM MBP for 30 min at 23 °C. The excess MBP was quenched by addition of 10 mM dithiothreitol, and the samples were irradiated with a long-wavelength ultraviolet lamp for 5 min at 4 °C. The samples were applied to a 10% acrylamide gel and subjected to SDS−PAGE according to the method of Laemmli (*45*). Proteins were then transferred to nitrocellulose, and Western blotting was perfomed using antibodies against Vma2p (subunit B) or Vma10p (subunit G) as described in the Experimental Procedures. Indicated to the left of each panel are the molecular masses of marker proteins and to the right the positions of subunits B and G and the predicted migration position for a B−G heterodimer. The positions of the B−E heterodimer reported previously (*42*) are also indicated.

results are consistent with our previous report indicating that subunit E could be cross-linked to sites on the outer surface of subunit B, both near the top and near the bottom of V_1 (*42*). Together, these results suggest that subunits E and G likely form part of a peripheral stalk connecting the V_1 and V_0 domains. This peripheral stalk can be visualized in electron micrographs of the V-ATPase complex (*39*, *40*) and, by analogy with the F-ATPases, is postulated to function as a stator to prevent rotation of the V_1 domain relative to subunit a in V_0 during ATP-induced rotation of the central stalk. In the F-ATPases, the peripheral stalk contains the δ subunit, which is located near the top of the complex (*27*), and the soluble portions of the b subunits, which extend a considerable distance perpendicular to the membrane (*28*). Our current results suggest that subunit G may correspond to the δ subunit of F_1 and subunit E to the soluble domain of the b subunit. On the other hand, the subunit stoichiometry (two copies of G per complex (*49*)) and the partial sequence homology between subunits G and b along one putative helical face (*51*) suggest that the G subunit may correspond to the b subunit homologue in the V-ATPases. This assignment is further supported by the ability to delete short stretches of both subunits without seriously compromising function, suggesting an extended flexible structure (*52*, *53*). It should also be noted that the lack of cross-linking of subunit G to cysteine residues located near the bottom of subunit B is not proof that these subunits are not in contact in this region. Additional structural data will be required to resolve this point.

Interaction between subunits E and G has been demonstrated by covalent cross-linking of these subunits in the bovine coated vesicle enzyme (*49*), by isolation of an E−G complex in yeast strains lacking various V-ATPase subunits (*54*, *55*) and by the lack of stability of subunit E in a strain lacking subunit G (*54*). From the current results we suggest that subunits E and G contact each other in the peripheral stalk of the V-ATPase. By contrast with subunits E and G, subunit D appears to be located within the interior of the V_1 complex, suggesting that subunit D is the most likely homologue to the γ subunit of the F-ATPases. The γ subunit of F_1 has been shown to undergo rotation during ATP hydrolysis (*32*−*34*) and to make contact with the ring of c subunits in F_0 (*25*, *56*). Thus, rotation of γ induces rotation of the c subunit ring during rotary catalysis (*35*−*37*). Our model (Figure 5 of ref *42*) places subunit D in the rotor part of the complex and postulates a central role for this subunit in coupling of ATP hydrolysis and proton translocation by the V-ATPases. Consistent with such a role in coupling is the observation that mutations can be isolated in subunit D that lead to altered coupling of proton transport and ATP hydrolysis (*57*). Moreover, these mutations cluster in two regions of the molecule near the N- and C-termini and appear to alter coupling in a synergistic manner, suggesting that subunit D may fold back upon itself in a hairpin coiled-coil structure similar to subunit γ of F_1 (*23*−*25*).

An interesting feature of the cross-linking between subunits B and D is the formation of multiple cross-linked products that are recognized by antibodies against both subunits (Figure 4). In particular, several cross-linked products with apparent molecular mass greater than 170 kDa are observed, and suggest that subunit D can be cross-linked to multiple B subunits in the same complex. Because there are three copies of subunit B per complex (*58*), the formation of such multimers is not surprising, particularly if subunit D is located within a central cavity surrounded by subunits A and B, as described above. In addition, the appearance of a pair of cross-linked products at the lowest molecular weight suggests that subunit B may be able to cross-link to subunit D at two different sites, giving rise to products of slightly different mobility. This result is again consistent with a hairpin structure for subunit D in which two different regions of the subunit could be in proximity to the same site in subunit B.

ACKNOWLEDGMENT

We thank Tsuyoshi Nishi, Shoko Kawasaki-Nishi, Elim Shao, and Takao Inoue for helpful discussions.

REFERENCES

1. Nishi, T., and Forgac, M. (2002) *Nat. Rev. Mol. Cell Biol. 3*, 94−103.
2. Forgac, M. (1999) *J. Biol. Chem. 274*, 12951−12954.
3. Graham, L. A., Powell, B., and Stevens, T. H. (2000) *J. Exp. Biol. 203*, 61−70.
4. Kane, P. M., and Parra, K. J. (2000) *J. Exp. Biol. 203*, 81−87.
5. Bowman, E. J., and Bowman, B. J. (2000) *J. Exp. Biol. 203*, 97−106.
6. Nelson, N., Perzov, N., Cohen, A., Hagai, K., Padler, V., and Nelson, H. (2000) *J. Exp. Biol. 203*, 89−95.
7. Futai, M., Oka, T., Sun-Wada, G., Moriyama, Y., Kanazawa, H., and Wada, Y. (2000) *J. Exp. Biol. 203*, 107−116.
8. Sze, H., Li, X., and Palmgren, M. G. (1999) *Plant Cell 11*, 677−690.
9. Li, Y.-P., Chen, W., Liang, Y., Li, E., and Stashenko, P. (1999) *Nat. Genet. 23*, 447−451.
10. Brown, D., and Breton, S. (2000) *J. Exp. Biol. 203*, 137−145.
11. Nanda, A., Brumell, J. H., Nordström, T., Kjeldsen, L., Sengelov, H., Borregaard, N., Rotstein, O. D., and Grinstein, S. (1996) *J. Biol. Chem. 271*, 15963−15970.
12. Wieczorek, H., Grüber, G., Harvey, W. R., Huss, M., Merzendorfer, H., and Zeiske, W. (2000) *J. Exp. Biol. 203*, 127−135.
13. Cross, R. L. (2000) *Biochim. Biophys. Acta 1458*, 270−275.
14. Weber, J., and Senior, A. E. (2000) *Biochim. Biophys. Acta 1458*, 300−309.
15. Fillingame, R. H., Jiang, W., and Dmitriev, O. Y. (2000) *J. Exp. Biol. 203*, 9−17.
16. Capaldi, R. A., Schulenberg, B., Murray, J., and Aggeler, R. (2000) *J. Exp. Biol. 203*, 29−33.
17. Futai, M., Omote, H., Sambongi, Y., and Wada, Y. (2000) *Biochim. Biophys. Acta 1458*, 276−288.
18. Yoshida, M, Muneyuki, E., and Hisabori, T. (2001) *Nat. Rev. Mol. Cell Biol. 2*, 669−677.
19. Zimniak, L., Dittrich, P., Gogarten, J. P., Kibak, H., and Taiz, L. (1988) *J. Biol. Chem. 263*, 9102−9112.
20. Bowman, B. J., Allen, R., Wechser, M. A., and Bowman, E. J. (1988) *J. Biol. Chem. 263*, 14002−14007.
21. Mandel, M., Moriyama, Y., Hulmes, J. D., Pan, Y. C., Nelson, H., and Nelson, N. (1988) *Proc. Natl. Acad. Sci. U.S.A. 85*, 5521−5524.
22. Hirata, R., Graham, L. A., Takatsuki, A., Stevens, T. H., and Anraku, Y. (1997) *J. Biol. Chem. 272*, 4795−4803.
23. Abrahams, J. P., Leslie, A. G., Lutter, R., and Walker, J. E. (1994) *Nature 370*, 621−628.
24. Bianchet, M. A., Hullihen, J., Pedersen, P. L., and Amzel, L. M. (1998) *Proc. Natl. Acad. Sci. U.S.A. 95*, 11065−11070.
25. Stock, D., Leslie, A. G., and Walker, J. E. (1999) *Science 286*, 1700−1705.
26. Aggeler, R., Haughton, M. A., and Capaldi, R. A. (1995) *J. Biol. Chem. 270*, 9185−9191.
27. Ogilvie, I., Aggeler, R., and Capaldi, R. A. (1997) *J. Biol. Chem. 272*, 16652−16656.
28. McLachlin, D. T., Bestard, J. A., and Dunn, S. D. (1998) *J. Biol. Chem. 273*, 15162−15168.
29. Birkenhager, R., Hoppert, M., Deckers-Hebestreit, G., Mayer, F., and Altendorf, K. (1995) *Eur. J. Biochem. 230*, 58−67.
30. Vik, S. B., and Antonio, B. J. (1994) *J. Biol. Chem. 269*, 30364−30369.
31. Junge, W., Sabbert, D., and Engelbrecht, S. (1996) *Ber. Bunsen-Ges. Phys. Chem. 100*, 2014−2019.
32. Duncan, T. M., Bulygin, V. V., Zhou, Y., Hutcheon, M. L., and Cross, R. L. (1995) *Proc. Natl. Acad. Sci. U.S.A. 92*, 10964−10968.
33. Sabbert, D., Engelbrecht, S., and Junge, W. (1996) *Nature 381*, 623−625.
34. Noji, H., Yasuda, R., Yoshida, M., and Kinoshita, K., Jr. (1997) *Nature 386*, 299−302.
35. Sambongi, Y., Iko, Y., Tanabe, M., Omote, H., Iwamoto-Kihara, A., Ueda, I., Yanagida, T., Wada, Y., and Futai, M. (1999) *Science 286*, 1722−1724.
36. Hutcheon, M. L., Duncan, T. M., Ngai, H., and Cross, R. L. (2001) *Proc. Natl. Acad. Sci. U. S. A. 98*, 8519−8524.
37. Tsunoda, S. P., Aggeler, R., Yoshida, M., and Capaldi, R. A. (2001) *Proc. Natl. Acad. Sci. U.S.A. 98*, 898−902.
38. Wilkens, S., and Capaldi, R. A. (1998) *Nature 393*, 29.
39. Boekema, E. J., Ubbink-Kok, T., Lolkema, J. S., Brisson, A., and Konings, W. N. (1997) *Proc. Natl. Acad. Sci. U.S.A. 94*, 14291−14293.
40. Wilkens, S., Vasilyeva, E., and Forgac, M. (1999) *J. Biol. Chem. 274*, 31804−31810.
41. Vasilyeva, E., Liu, Q., MacLeod, K. J., Baleja, J. D., and Forgac, M. (2000) *J. Biol. Chem. 275*, 255−260.
42. Arata, Y., Baleja, J. D., and Forgac, M. (2002) *J. Biol. Chem. 277*, 3357−3363.
43. Liu, Q., Kane, P. M., Newman, P. R., and Forgac, M. (1996) *J. Biol. Chem. 271*, 2018−2022.
44. Yamashiro, C. T., Kane, P. M., Wolczyk, D. F., Preston, R. A., and Stevens, T. H. (1990) *Mol. Cell Biol. 10*, 3737−3749.
45. Laemmli, U. K. (1970) *Nature 227*, 680−685.
46. Drose, S., Bindseil, K. U., Bowman, E. J., Siebers, A., Zeeck, A., and Altendorf, K. (1993) *Biochemistry 32*, 3902−3906.
47. Bradford, M. M. (1976) *Anal. Biochem. 72*, 248−254.
48. Kane, P. M., Kuehn, M. C., Howald-Stevenson, I., and Stevens, T. H. (1992) *J. Biol. Chem. 267*, 447−454.
49. Xu, T., Vasilyeva, E., and Forgac, M. (1999) *J. Biol. Chem. 274*, 28909−28915.
50. Dormán, G., and Prestwich, G. D. (1994) *Biochemistry 33*, 5661−5673.
51. Hunt, I. E., and Bowman, B. J. (1997) *J. Bioenerg. Biomembr. 29*, 533−540.
52. Sorgen, P. L., Caviston, T. L., Perry, R. C., and Cain, B. D. (1998) *J. Biol. Chem. 273*, 27873−27878.
53. Charsky, C. M. H., Schumann, N. J., and Kane, P. M. (2000) *J. Biol. Chem. 275*, 37232−37239.
54. Tomashek, J. J., Graham, L. A., Hutchins, M. U., Stevens, T. H., and Klionsky, D. J. (1997) *J. Biol. Chem. 272*, 26787−26793.
55. Tomashek, J. J., Garrison, B. S., and Klionsky, D. J. (1997) *J. Biol. Chem. 272*, 16618−16623.
56. Watts, S. D., Tang, C., and Capaldi, R. A. (1996) *J. Biol. Chem. 271*, 28341−28347.
57. Xu, T., and Forgac, M. (2000) *J. Biol. Chem. 275*, 22075−22081.
58. Arai, H., Terres, G., Pink, S., and Forgac, M. (1988) *J. Biol. Chem. 263*, 8796−8802.

BI0262449